

CHAPTER TWO : LITERATURE REVIEW

Many researches had been conducted to study OISF. The creation of mechanical damages on wafer prior to oxidation was by abrasion or coarse slurry polishing. Models were proposed since 1960s to explain OISF growth mechanism. Booker and Tunstall [13, 15] have carried out detail contrast analysis of OISF structure in niobium-containing autenitic stainless steel. They suggested that the precipitation of silicon dioxide (SiO_2) is accompanied by a volume change, leading to the gliding of Schockley partial and emission of vacancies from the Frank partial. This results in the growth of the Frank partial and hence in the formation of the stacking fault that is extrinsic in nature.

Alternatively Sanders and Dobson [17] found that precipitation is not a prerequisite for propagation of the Frank partial [16, 17]. They studied fault growth phenomenon in silicon by annealing thin foils used for electron microscopy. No precipitation was detected in the faults, which grow when annealed in air and shrink upon vacuum annealing. They believed that fault growth anisotropy is a consequence of vacancy imbalance in material. Reduced vacancy concentration at surface will promote greater growth rate near the surface because growth of extrinsic OISF [16,18] occurs by vacancy emission.

Lawrence [20], Fisher and Amick [21] believed that surface mechanical damage [16, 18] is a requirement for fault nucleation. For them, uniform defect length [7, 20, 21, 23] observed on (100), (110) and (111) planes, is the characteristic of OISF formed on mechanically damaged wafer. However Joshi [22] demonstrated

that faults can be formed in damage-free silicon surface and proposed that silicon oxide precipitates in material can be the nucleation centers for faults.

Lawrence [20] suggested that fault nucleation required crevices in the as polished wafer surfaces, high annealing temperature, and a furnace with oxidizing ambient. Fault nucleation sites for diamond-polished wafers were found localized at $300 \pm 50 \text{ \AA}$ nearest to polished wafers surface. Fault size maintained but density reduces as depth from surface increases. Therefore factors that govern fault growth were not so localized. Size of a SF is governed by strain in the wafer lattice, surface oxide growth, and oxidation time and temperature. Prolonged annealing and introduction of stress to a faulted lattice by diffusion of solute into silicon were found to annihilate SFs.

Murarka and Quintana [10] also detected uniformity in length for OISF formed, regardless of wafer orientation and dopant used. The length of 95% of OISFs formed is uniform but the remaining 5% showed very wide length distribution. The distribution of the 5% non-uniform length for n-type wafers is about an order of magnitude higher than the length distribution of p-type wafers. Uniform length for both n and p-types are comparable. They claimed that n-type wafer may have more nucleation sites on the surface or they required lower driving force, leading to easier nucleation and growth of faults. Uniform length suggests that these OISFs are all heterogeneously nucleated at surface from the same source and at the same time during oxidation.

Length of OISF, L , for Czochralski wafer oxidized in 100% oxygen at various temperatures is given by [2, 4, 10]

$$L(\mu\text{m}) = A t^n \exp(-Q/kT)$$

where Q , t , n , k , A and T are the activation energy of OISF growth, oxidation time, number exponent, Boltzmann constant, constant value and absolute temperature respectively. The number exponent of silicon is approximately 0.8 while the activation energy for OISF growth is around 2.3eV, irrespective of oxidation ambient and crystal orientation of substrates. For the 5% OISFs having huge fluctuation in length, no correlation was found between that SF length and the oxidation time and temperature.

Fisher and Amick [21] studied the effect of oxidation time and Sirtl etching time to OISF formation using (100), (110) and (111) wafers. They found that OISF density on (111) wafer is independent of oxidation time. Uniform OISF length was also observed but the length increases with oxidation time. With further etching, OISF broaden but not lengthen. Besides OISF from all surface orientation sometimes meet but apparently never cross. From this they concluded that during growth, if one end of a line approaches another line lying across its path, further growth of that end ceases since such a fault could not propagate easily through a SF lying in a different (111) plane. Therefore such OISF is shorter than those unobstructed OISFs.

Hu [4] explained crystal orientation dependence of OISF formation using a model envisages a small incompleteness of oxidation that produces interstices. As

interstices saturate the lattice, they will undergo surface regrowth. Surface regrowth is basically analogous to the vapor-growth phenomenon. The only difference being that in the usual vapor-growth process the adatoms come from vapor phase, whereas in the surface regrowth the atoms come from the interstices of either substrate or, the oxide film.

The rate of surface regrowth is proportional to the density of surface kinks (*Refer Figure 2.1 and Figure 2.2*), which is in turn dependent on the surface orientation. Surface regrowth will reduce interstices available for OISF formation. OISF will be formed by precipitation of excess interstices after undergone surface regrowth at nucleation sites. Since surface kink density is dependent of crystal orientation, therefore OISF density must be dependent of crystal orientation too.

Due to surface kinks will reduce silicon interstices density to lower level, homogeneous nucleation is not possible but heterogeneous nucleation [23] is applicable. Heterogeneous nucleation process happens within very short time at the early stage of oxidation, usually less than one second, this leads to uniform SF size. The occasionally observed variation in the size of bulk-SF is attributed to a continuous formation of SF nuclei.

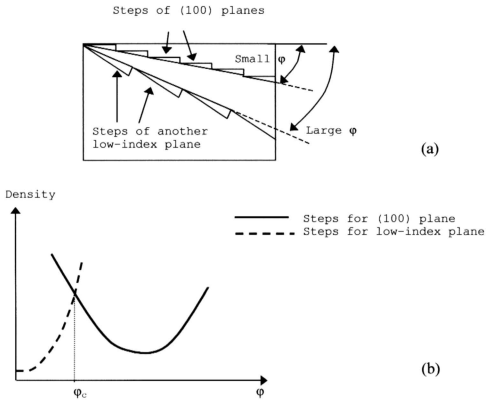


Figure 2.1 : (a) Switchover of constituting surface steps from one low index-plane to another as ϕ increases beyond some critical angle ϕ_c and (b) Density of surface kinks as a function of angle ϕ deviating from a (100) plane towards, say a $\langle 010 \rangle$ direction.

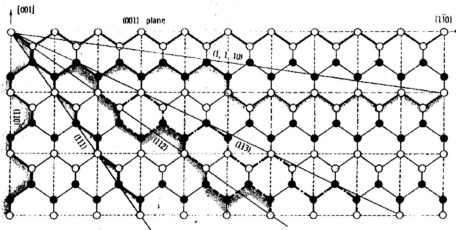


Figure 2.2 : Surface kinks on wafer surface with different surface orientation.

Both growth rate and the shrinkage rate of OISF are independent of the fault size. Therefore it is a reaction-controlled mechanism rather than a diffusion-controlled mechanism. The activation energy of growth is 2.3eV. This value does not depend on oxidation ambient, or on substrate surface orientation. Backside gettering (using e.g. mechanical lapping, polycrystalline silicon film, etc.) is often greatly reduces the density of OISF.

Ravi and Varker [3] studied both damaged surface and damage-free silicon wafer employing surface etching techniques and TEM. They proposed that extra surface area at a mechanically damaged point causes local reduction in the vacancies, leading to the precipitation of excess self-interstitial in the form of extrinsic SFs. Relative size of OISF over large area is uniform, indicating common origin of all the defects [3, 20, 21]. OISF from damage-free surface is independent of orientation and crystal growing technique (Czochralski grown or Float Zone (FZ) grown) [3] but its size and density is a function of oxide thickness. Therefore fault formation is a dynamic phenomenon with new faults being nucleated continuously as oxidation proceeds.

Thomas [23] believed that OISF formation depends on the purity of silicon used. In the case where a (111) plane is parallel to the surface, stress relief may be accomplished without the dislocation moving out of this plane. In highly doped specimens ($<0.001\Omega\text{cm}$, (111) oriented) and specimen heated with copper, no stacking fault is observed after annealing at 1150°C. Dislocations introduced during polishing rearranged during annealing and formed networks which lie parallel to the surface suppressed stacking fault formation. For materials with

slightly higher resistivity, some faults are produced but the number and size are smaller than in purer material. The reason for this phenomenon is not known.

Another researcher, Mayer [19], observed change in defect size and appearance as etching proceeds from 1 minute to 12 minutes. OISFs formed were raised above background surface by up to 12 μm in width at the middle point. Removed surface damages can be re-introduced by repeating polishing (abrasion) and OISF density twice as high as normal can be obtained by re-oxidized those oxidized wafer having its oxide stripped with HF.

Longer OISF was found on wafer oxidized in dry oxygen compared to steam. Mayer [19] suggested that OISF formation is a diffusion or precipitation phenomenon. He believed in the “discreteness of sites” in defect areas. Discrete sites have different reactivity because of a strain field arising from localized clustering of oxygen atoms around the lattice strain or mismatch point. These defects can break up into several discrete portions. Therefore reduction in OISF size and increment of OISF density in argon annealing was observed.

Murarka and Quintana [10] detected increment in OISF density when etching time increases. In some cases the increment can be as high as 50%. Besides OISF density is a function of depth, OISF length distribution on wafer surface was found on deeper etched surface. Size variation both on surface and deeper surface from oxide-silicon interface could be due to perturbations during crystal growth or due to lattice damage introduced during wafer sawing and polishing.

Sugita et al. [9] reported the relationship between faulted defect generation and surface orientation of oxidized specimens having several degrees off the [100] axis. When surface orientation deviation is 0° , OISFs observed are orthogonal to each other. When deviation angle, $\theta \sim 3^\circ$, OISF from two of the four $\{111\}$ planes disappeared, all OISFs observed are all parallel to one another. When θ is at $3^\circ \sim 9^\circ$, no OISF was observed. However all OISF reappeared as “V” patterned when θ increased to 10° .

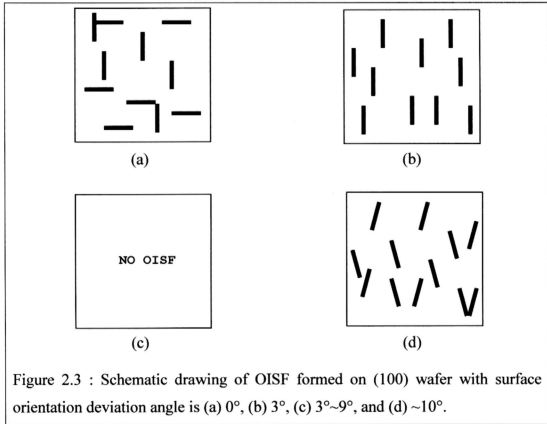


Figure 2.3 : Schematic drawing of OISF formed on (100) wafer with surface orientation deviation angle is (a) 0° , (b) 3° , (c) $3^\circ \sim 9^\circ$, and (d) $\sim 10^\circ$.

X-ray topography employed had proven that the disappearance of OISF implied the disappearance of faulted defects. They speculated that defect structure seems to be related to surface structure, including the interface structure, of silicon that is associated with strain centers or a minute amount of contamination.

Rozgonyi et al. [8], while studying on whether dislocation is required for OISF formation, demonstrated that the source of OISF in the bulk of {100}-oriented CZ wafers is impurity precipitate which can be identified before oxidation as a hillock etch feature. They believed that OISF formation proceeds via a stress-enhanced super-saturation of interstitial. No dislocation is required [8, 27].

Later in 1995, Marsden et al. [6] discovered that OISF ring formation on dislocation-free wafer depends on the radial distribution of bulk micro damage (BMD) determined by the pre-annealing condition before oxidation. The ability for these BMDs to grow during pre-annealing to nucleate OISFs with subsequent oxidation is determined by the strain surrounding them. However to realize OISF nucleation, the strain must lie within specific limits controlled by the size of the BMD.

Table 2.1 shows the summary of some of the researcher's findings over years. The researches included are those related to OISF density study using wafer with different surface orientation, oxidation ambient and oxidation temperature. Some of them even looked into activation energies required for OSIF formation and try to calculation the exponent number, n , using empirical results obtained.

Table 2.1 : Some of the Researches Done on OISF in Silicon [10]

Reference (Published year)	Material Description	Oxidation Condition	OISF Density	n	Q (eV)
Thomas [23] (1963)	(111)	Air, 1150°C	10^6	0.82^f	-
Queinsser and van Loon [7] (1964)	(100)	Steam, 1100-1300°C Air, 1100-1300°C	$5 \times 10^4^e$ $5 \times 10^4^e$	1.0^e $0.8-0.9^e$	0.25 1.6
Fisher and Amick [21] (1966)	n and p-type : (100), (110), and (111)	Steam, 1050-1250°C	10^7^a , 10^4^b	0.8	~ 2
Lawrence [20] (1969)	n and p-type (111)	Steam, 1150°C Air, 1150°C	$10^3 - 10^7$ -	- -	- -
Sanders and Dobson [17] (1969)	n and p-type (111)	Air, 1050-1250°C	High density	-	2.1 ± 0.2
Mayer [19] (1970)	n and p-type (100)	Steam, 1100°C	$2-8 \times 10^5$	0.62^d	-
Sugita et al. [9] (1971)	n-type (100)	Wet, 1200°C	$10^4 - 10^5$	-	-
Osburn and Ormond [24] (1974)	n-type (100)	Wet, 1000°C	$10^4 - 10^5$	-	-
Ravi and Varker [3] (1974)	(100), (111)	Steam, 1100°C	$5.5-15 \times 10^3$	-	-
S. M. Hu [29] (1975)	p-type (100), (1,0,11), (111)	Steam, 1050-1300°C Dry, 1100-1250°C	10^4 , 10^5^e -	- 0.8	2.3 2.3
Murarka and Quintana [10] (1977)	n-type (100) p-type (100)	Steam, Dry 1000- 1200°C Steam, 1000-1200°C Dry, 1000-1200°C	$10^3 - 10^6$ 50-1000 50-1000	- 0.66 0.85	- 2.3 2.5

REMARK :

n = Exponent Number

Q = Activation Energy

OISF Density unit = counts/cm²

- ^a On mechanically polished wafers
 - ^b On chemically polished wafers
 - ^c Calculated by use of Hu's Figs. 1(a) and 2 for (100) silicon
 - ^d Least-squares fit of Mayer's data (his table 3). Dry oxidation times appear to be misprinted and hence not considered
 - ^e Calculated from Queisser and van Loon's Fig. 1 and 2
 - ^f Least-squares fit of Thomas's data (his Table 1)
-